J. Plasma Physics (2011), *vol.* 77, *part* 5, *pp.* 663–673. © Cambridge University Press 2011
doi:10.1017/S0022377811000055

The optimum shielding around a test charge in plasmas containing two negative ions

W. M. MOSLEM[1]†, R. SABRY[2]‡ and P. K. SHUKLA[3]§

[1]Department of Physics, Faculty of Science, Port Said University, Port Said, Egypt (wmmoslem@hotmail.com)

[2]Theoretical Physics Group, Department of Physics, Faculty of Science, Mansoura University, Damietta Branch, New Damietta 34517, Egypt

[3]RUB International Chair, International Center for Advanced Studies in Physical Sciences, Faculty of Physics & Astronomy, Ruhr University Bochum, D-44780 Bochum, Germany

(Received 29 November 2010 and accepted 15 January 2011; first published online 15 February 2011)

Abstract. This paper focuses on the progress in understanding the shielding around a test charge in the presence of ion-acoustic waves in multispecies plasmas, whose constituents are positive ions, two negative ions, and Boltzmann distributed electrons. By solving the linearized Vlasov equation with Poisson equation, the Debye–Hückel screening potential and wakefield (oscillatory) potential distribution around a test charge particle are derived. It is analytically found that both the Debye–Hückel potential and the wakefield potential are significantly modified due to the presence of two negative ions. The present results might be helpful to understand and to form new materials from plasmas containing two negative ions such as $Xe^+ - F^- - SF_6^-$ and $Ar^+ - F^- - SF_6^-$ plasmas, as well as to tackle extension of the test charge problem in multinegative ions' coagulation/agglomeration.

1. Introduction

For more than four decades, negative ion plasmas attracted attention due to their importance both in laboratory experiments and in space plasma observations [1–15]. Therefore, the importance of negative ion plasmas to the field of plasma physics is growing. To treat such plasmas skillfully, basic study and development of diagnostic techniques on negative ion plasmas is indispensable. In a negative ion plasma, the number of electrons decreases according to the charge neutrality, i.e. $n_e = n_+ - n_-$,

† Also at: International Center for Advanced Studies in Physical Sciences, Faculty of Physics & Astronomy, Ruhr University Bochum, D-44780 Bochum, Germany (wmmoslem@hotmail.com, wmm@tp4.rub.de)

‡ Also at: International Center for Advanced Studies in Physical Sciences, Faculty of Physics & Astronomy, Ruhr University Bochum, D-44780 Bochum, Germany (sabryphys@yahoo.com, sabry@tp4.rub.de)

§ Also at: Institut für Theoretische Physik, Fakultät für Physik und Astronomie, Ruhr-Universität Bochum, D-44780 Bochum, Germany; Department of Physics, Umeå University, SE-90187 Umeå, Sweden; Max-Planck-Institut für extraterrestrische Physik, D-85741 Garching, Germany; GoLP/Instituto Superior Técnico, 1049-001 Lisbon, Portugal; CCLRC Centre for Fundamental Physics, Rutherford Appleton Laboratory, Chilton, Didcot, Oxon 0X11 0QX, UK; SUPA Department of Physics, University of Strathclyde, Glasgow G 40NG, UK; School of Physics, Faculty of Science & Agriculture, University of Kwazulu-Natal, Durban 4000, South Africa (ps@tp4.rub.de)

https://doi.org/10.1017/S0022377811000055 Published online by Cambridge University Press

where n_e, n_+, and n_- are the electron, positive ion, and negative ion densities, respectively. The resulting decrease in the shielding effect produced by electrons, which is one of the main effects governing the behavior of plasmas, characterizes the specific phenomena of negative ion plasmas. From this perspective, it seems to follow that the negative ions only influence plasmas secondarily. Although this is a fact, most of the phenomena are actually affected by the negative ions themselves as well as by the lack of electrons [16]. Indeed, negative ion plasmas have been extensively studied in the past years by many authors (see, e.g. [17–22]). Motivated by the experimental studies of multicomponent plasmas with positive–negative ions in Q-machines and double plasma devices, Ichiki et al. [23] have studied the propagation of ion-acoustic waves in multiion plasmas including two negative ion species. The characteristic behavior of the ion-acoustic waves in $Xe^+ - F^- - SF_6^-$ and $Ar^+ - F^- - SF_6^-$ plasmas was investigated both experimentally and theoretically. Furthermore, Cassini spacecraft has conclusively demonstrated the presence of many types of heavy negative ions in the upper region of Titan atmosphere [24]. These particles may act as organic building blocks for even more complicated molecules.

The electrostatic potentials dealing with the passage of charged particles through the plasma have been presented in an elegant paper by Neufeld and Ritchie [25]. They calculated the potential distributions of a test particle in an electron plasma with fixed ion background and pointed out their importance to energy loss. The test charge potential calculation has been further extended by Sanmartin and Lam [26] and by Chen et al. [27] by incorporating the ion dynamics. The latter allows the possibility of far-wake structures in rarefied plasma flows past charged bodies. The concept of the oscillatory wakefield due to a test charge was first introduced by Nambu and Akama [28] in an unmagnetized electron–ion plasma. Physically, it is well known that a stationary test charge polarizes the plasma medium and is shielded by the opposite polarity charges. The motion of a test charge leads to polarization of the plasma medium, i.e. an oscillatory wakefield is generated behind the test charge when the test charge speed resonates with the phase speed of the plasma wave. On the other hand, when the speed of the test charge equals the phase speed of plasma oscillations, an oscillatory wakefield is formed behind the test charge, which is responsible for attracting charged particles of opposite polarity. This wakefield contains both positive and negative potential regions, depending strongly on the test charge speed, which slowly damps for several Debye lengths. For higher test charge speeds, the wakefield is further pronounced. In the negative potential region, the positive ions can be trapped, and there appears an attractive force between the same polarity charges (e.g. the electrons and negative ions).

During the last decades, a test charge problem has received a great deal of attention of the plasma community in the context of their applications in many plasma phenomena taking into account the effect of the dust charge particles and dynamics of either electrons or ions in unmagnetized and magnetized plasmas; see, for example [29–34]. In view of the crucial importance of the test charge problem applications, such as in the acceleration of particles, in the formation of the dust particles into regular crystalline structures in dusty plasmas, and in the coagulation of small dust particles in space and astrophysical plasmas, etc., there is a need for investigating the behavior of test charge particles in the presence of two/different kinds of negative ions as presented experimentally [23] and observed in space [24]. Therefore, the goal of the present work is to tackle extension of the electrostatic asymmetric shielding

https://doi.org/10.1017/S0022377811000055 Published online by Cambridge University Press

potential and consequent generation of the dynamical oscillatory wakefield potential in a plasma composed of four distinct particle populations, namely positive ions, two negative ions, and isothermal electrons. Particular questions to be answered are, e.g. (i) could the negative ion species play a role on the shielding potential and the oscillatory wakefield potential profiles, and (ii) whether the negative ion parameters and electron-to-ion temperature ratio can modify the trajectories of the wakefield potential profile. The results from this work are expected to contribute to the in-depth understanding of the charged particle repulsion and attraction in experimental plasmas and in space plasmas in general.

The paper is organized in the following fashion: In Sec. 2, both linearized Vlasov equation and Poisson equation are presented to calculate the Debye–Hückel and wakefield potentials for a test charge in multicomponent plasma containing two negative ion species. The numerical results are discussed in Sec. 3 and summarized in Sec. 4.

2. Dispersion relation and potential distribution

Let us consider an unmagnetized collisionless multicomponent plasma consisting of positive ions, two negative ion species, and Boltzmann electrons. The equilibrium charge neutrality condition reads $n_i^{(0)} = n_1^{(0)} + n_2^{(0)} + n_e^{(0)}$, where $n_j^{(0)}$ is the equilibrium number density of jth species (j equals to e for electrons, i for positive ions, 1 for first negative ions, and 2 for second negative ions). The dynamics of such a multicomponent plasma can be described by the linearized Vlasov equation

$$(\partial_t + \mathbf{V}\cdot\nabla) f_{j1} + \frac{q_j}{m_j}\mathbf{E}_1\cdot\nabla_{\mathbf{v}} f_{j0}(\mathbf{V}) = 0, \tag{1}$$

where f_{j1} ($\ll f_{j0}$) is the perturbed (unperturbed) particle distribution function, and q_j and m_j are the charge and mass, respectively. $\nabla = \hat{\mathbf{e}}_x\partial/\partial X + \hat{\mathbf{e}}_y\partial/\partial Y + \hat{\mathbf{e}}_z\partial/\partial Z$, and $\nabla_{\mathbf{v}} = \hat{\mathbf{e}}_x\partial/\partial V_x + \hat{\mathbf{e}}_y\partial/\partial V_y + \hat{\mathbf{e}}_z\partial/\partial V_z$, where $\hat{\mathbf{e}}_x$, $\hat{\mathbf{e}}_y$, and $\hat{\mathbf{e}}_z$ are the unit vectors along the x-, y-, and z-axes, respectively. Here, $\mathbf{E}_1 (= -\nabla\varphi_1)$ is the induced electric field with the electrostatic potential φ_1. Equation (1) is coupled through Poisson equation by the perturbed distribution function f_{j1}, as

$$\begin{aligned}\nabla^2\varphi_1 &= -4\pi(\rho_{\text{plasma}} + \rho_{\text{test}})\\ &= -4\pi\sum_j q_j\int f_{j1}\mathrm{d}\mathbf{V} - 4\pi Q_p\delta(\mathbf{r} - \mathbf{V}_p t),\end{aligned} \tag{2}$$

where ρ_{plasma} represents the charge density of the plasma particles, i.e. positive ions, two negative ion species, and electrons, ρ_{test} is the test charge density, and Q_{p} is the charge of the test particle propagating through the plasma with a constant velocity $\mathbf{V}_{\text{p}}$ along the z-axis. Here, $\delta(\mathbf{r} - \mathbf{V}_{\text{p}}t)$ is the three-dimensional Dirac delta function. The test charge can be assumed to be at rest at origin in a steady state plasma for $\mathbf{V}_{\text{p}} = 0$.

Applying space–time Fourier transformations, (1) and (2) can be combined as

$$\tilde{\varphi}_1(\mathbf{k},\omega) = \frac{8\pi Q_p\delta(\omega - \mathbf{k}\cdot\mathbf{V}_p)}{k^2\varepsilon(k,\omega)}, \tag{3}$$

https://doi.org/10.1017/S0022377811000055 Published online by Cambridge University Press

where ω and $\mathbf{k}$ are the wave frequency and wavevector, respectively, and $\varepsilon(k,\omega)$ is the dielectric constant given by

$$\varepsilon(k,\omega) = 1 + \sum_j \frac{K_{Dj}^2}{k^2} W(C_j). \tag{4}$$

In (4), $W(C_j)$ is the plasma dispersion function [28] given by

$$W(C_j) = (1/\pi)^{1/2} \int_{-\infty}^{\infty} \frac{q \exp(-q^2/2)}{q - C_j} \mathrm{d}q,$$

where $C_j = \omega/k_z V_{\mathrm{t}j}$, $V_{\mathrm{t}j}$ is the thermal speed, and K_{Dj} is the Debye wavenumber which is actually the inverse of the Debye length $\lambda_{D\mathrm{e}}(= \sqrt{T_{\mathrm{e}}/4\pi e^2 n_{\mathrm{e}}^{(0)}})$.

For ion-acoustic waves, we have $V_{\mathrm{ti},1,2} \ll \frac{\omega}{k} \ll V_{\mathrm{te}}$. Therefore, the plasma dispersion function gives $W(C_{\mathrm{e}}) = 1$, $W(C_i) = -1/2C_i^2$, $W(C_1) = -1/2C_1^2$, and $W(C_2) = -1/2C_2^2$, for electrons, positive ions, first negative ions, and second negative ions, respectively. Using the plasma dispersion functions with (4), the reciprocal of the dielectric constant given by

$$\frac{1}{\varepsilon(k,\omega)} = \frac{k^2\lambda_{\mathrm{De}}^2}{k^2\lambda_{\mathrm{De}}^2 + 1}\left(1 + \frac{\omega_k^2}{\omega^2 - \omega_k^2}\right), \tag{5}$$

where

$$\omega_k^2 = \frac{\left(\omega_{pi}^2 + \omega_{p1}^2 + \omega_{p2}^2\right) k^2\lambda_{\mathrm{De}}^2}{1 + k^2\lambda_{\mathrm{De}}^2} \tag{6}$$

is the dispersion relation of the ion-acoustic waves which is now modified with the first (second) negative ion plasma frequency $\omega_{\mathrm{p}1(2)} = (4\pi e^2 n_{1(2)}^{(0)}/m_{1(2)})^{1/2}$. Here, $\omega_{\mathrm{p}i} = (4\pi e^2 n_i^{(0)}/m_i)^{1/2}$ is the positive ion plasma frequency, $m_{i,1,2}$ are the masses of the positive, first and second negative ions. $\lambda_{D\mathrm{e}} = (T_{\mathrm{e}}/4\pi e^2 n_{\mathrm{e}}^{(0)})^{1/2}$ is the electron Debye length.

Taking the inverse space–time Fourier transformation to (3), we can express the electrostatic potential at an arbitrary position $\mathbf{r}$, as

$$\varphi_1(\mathbf{r},t) = \frac{Q_{\mathrm{p}}}{2\pi^2} \int \frac{\mathrm{d}\mathbf{k}}{k^2} \frac{\exp[i\mathbf{k}\cdot(\mathbf{r} - \mathbf{V}_{\mathrm{p}}t)]}{\varepsilon(k, \mathbf{k}\cdot\mathbf{V}_{\mathrm{p}})}. \tag{7}$$

Substituting (5) into (7), the Debye–Hückel and wakefield potentials, respectively, become

$$\varphi_D(\mathbf{r},t) = \frac{Q_{\mathrm{p}}}{2\pi^2} \int \mathrm{d}\mathbf{k} \left(\frac{\lambda_{D\mathrm{e}}^2}{k^2\lambda_{D\mathrm{e}}^2 + 1}\right) \exp[i\mathbf{k}\cdot(\mathbf{r} - \mathbf{V}_p t)], \tag{8}$$

and

$$\varphi_W(\mathbf{r},t) = \frac{Q_{\mathrm{p}}}{2\pi^2} \int d\mathbf{k} \left(\frac{\lambda_{D\mathrm{e}}^2}{k^2\lambda_{D\mathrm{e}}^2 + 1}\right) \frac{\omega_k^2}{(\mathbf{k}\cdot\mathbf{V}_{\mathrm{p}})^2 - \omega_k^2} \exp[i\mathbf{k}\cdot(\mathbf{r} - \mathbf{V}_{\mathrm{p}}t)]. \tag{9}$$

We shall use the spherical polar coordinates to simplify (8), by using $\mathbf{k} = (k\sin\theta_k \cos\varphi_k,\ k\sin\theta_k \sin\varphi_k,\ k\cos\theta_k)$, $\mathbf{r} = (r\sin\theta_r\cos\varphi_r,\ r\sin\theta_r\sin\varphi_r,\ r\cos\theta_r)$, and $\mathbf{V}_{\mathrm{p}} = (0,0,V_{\mathrm{p}})$, so that $\mathbf{k}\cdot(\mathbf{r} - \mathbf{V}_{\mathrm{p}}t) = k\rho\sqrt{1-\mu^2}\cos\varphi_k + k\mu Z$, where $\rho(= r\sin\theta_r)$ and $Z(= r\cos\theta_r - V_{\mathrm{p}}t)$ are the radial and axial distances of a test charge from an observation point $\mathbf{r}$, $\mu = \cos\theta_k$, and $\sin\theta_k = \sqrt{1-\mu^2}$. After some algebraic manipulations, the

https://doi.org/10.1017/S0022377811000055 Published online by Cambridge University Press

modified Debye–Hückel potential takes the following form:

$$\varphi_D = \frac{Q_p}{r}\exp\left(-\frac{r}{\lambda_{De}}\right), \tag{10}$$

where $r = (\rho^2 + Z^2)^{1/2}$.

To derive an analytical expression for ϕ_W, it convenient to use the cylindrical co-ordinates, and then expressing $\mathbf{k}\cdot(\mathbf{r} - \mathbf{V}_p t) = k_\perp \rho\cos\varphi_k + k_\parallel \xi$ and $d\mathbf{k} = k_\perp dk_\perp k_\parallel d\varphi_k$ to obtain

$$\phi_W(\rho, Z) = \frac{Q_p}{\pi\lambda_{De}}\int \frac{K_\perp dK_\perp dK_\parallel J_0[K_\perp\rho/\lambda_{De}]}{K_\perp^2 + K_\parallel^2 + 1}\exp\left(\frac{iK_\parallel Z}{\lambda_{De}}\right)$$

$$\times \frac{(K_\perp^2 + K_\parallel^2)(\omega_{pi}^2 + \omega_{p1}^2 + \omega_{p2}^2)\lambda_{De}^2}{(K_\parallel^2 - K_+^2)(K_\parallel^2 + K_-^2)V_p^2}. \tag{11}$$

Here, $Z = r_\parallel - V_p t$, $K_\parallel$, and $K_\perp$ are the parallel and perpendicular components of the normalized wavenumber $K(= k\lambda_{De})$, J_0 is the zeroth-order Bessel function which tends to unity for small argument, i.e. for $K_\perp\rho/\lambda_{De} < 1$. Equation (11) represents the wakefield potential generated from the residues at the poles $K_\parallel = \pm K_+$, where $K_\pm^2$ can be defined as

$$K_\pm^2 = \mp\frac{1}{2}\left[1 + K_\perp^2 - \frac{(\omega_{pi}^2 + \omega_{p1}^2 + \omega_{p2}^2)}{V_p^2}\lambda_{De}^2\right]$$

$$+ \frac{1}{2}\sqrt{\left[1 + K_\perp^2 - \frac{(\omega_{pi}^2 + \omega_{p1}^2 + \omega_{p2}^2)}{V_p^2}\lambda_{De}^2\right]^2 + \frac{2(\omega_{pi}^2 + \omega_{p1}^2 + \omega_{p2}^2)}{V_p^2}K_\perp^2\lambda_{De}^2}. \tag{12}$$

For $K_\perp^2 \ll 1, K_-$ and K_+ may be approximated, respectively, as

$$K_- \approx \left[1 - \frac{(\omega_{pi}^2 + \omega_{p1}^2 + \omega_{p2}^2)}{V_p^2}\lambda_{De}^2\right]^{1/2}, \tag{13}$$

and

$$K_+ \approx \frac{(\omega_{pi}^2 + \omega_{p1}^2 + \omega_{p2}^2)^{1/2}}{V_p}K_\perp\lambda_{De}. \tag{14}$$

Using (13) and (14) in (11) and integrating over $K_\parallel$ and $K_\perp$, we obtain the main contribution of φ_W as

$$\varphi_W(Z, t) = \frac{2Q_p}{Z}\left[1 + \frac{(\omega_{pi}^2 + \omega_{p1}^2 + \omega_{p2}^2)}{V_p^2}\lambda_{De}^2\right]\left[1 - \frac{(\omega_{pi}^2 + \omega_{p1}^2 + \omega_{p2}^2)}{V_p^2}\lambda_{De}^2\right]^{-1}$$

$$\times\cos\left(\frac{(\omega_{pi}^2 + \omega_{p1}^2 + \omega_{p2}^2)^{1/2}}{V_p}Z\right). \tag{15}$$

Equation (15) represents the wakefield potential of a test charge propagating with a constant speed along the z-axis, which is modified by the dynamics of two negative ion species. For neglecting the dynamics of the negative ions, we have $\omega_{p1,2}^2 = 0$,

https://doi.org/10.1017/S0022377811000055 Published online by Cambridge University Press

then the wakefield potential from (15) reduces to an expression involving only the dynamics of the positive ions as studied in [28].

3. Numerical results

To illustrate the usefulness of our model, we show two examples based on laboratory experiment by Ichiki et al. [23]. However, it is worth to give a glimpse of the conceptual as well as a brief description of this laboratory experiment. This experiment was an investigation to the ion dynamics (via ion-acoustic waves) in the presence of two negative ion plasmas, namely ($Xe^+-F^--SF_6^-$) and ($Ar^+-F^--SF_6^-$). Indeed, both types of plasmas have different masses, namely, m_1 is the mass of the first negative ion F^-, m_2 is the mass of the second negative ion SF_6^-, and m_i is the mass of the positive ion Xe^+ or Ar^+. Therefore, it is expected that the mass may play a role in the properties of the electrostatic potential, which is one of the motives to our study. The following density parameters shall be used for two negative ion plasmas, namely, $\alpha = (n_1^{(0)} + n_2^{(0)})/n_i^{(0)}$ the negative ion concentration and $v = n_2^{(0)}/(n_1^{(0)}+n_2^{(0)})$ the density rate of SF_6^-. The densities can be expressed using these notations as $n_i^{(0)} : n_e^{(0)} : n_1^{(0)} : n_2^{(0)} = 1 : 1-\alpha : \alpha(1-v) : \alpha v$. Furthermore, the effects of the total negative ion concentration α, density rate of the second negative ion v, and electron-to-ion temperature ratios ($\theta_{i,1,2} = T_e/T_{i,1,2}$) will be examined. Following the assumption of lchiki et al. [23], we assume that $\theta_i = \theta_1 = \theta_2 = \theta$ (i.e. $T_i = T_1 = T_2$). Note that θ's more than 1 are taken into account mainly because Landau damping is too strong to observe ion-acoustic waves for θ less than 1, and hence there is not much interest for this study.

For numerical analysis, we express (10) and (15) by using the normalized parameters such as $\widetilde{\varphi}_D = e\varphi_D/T_e$, $\widetilde{\varphi}_W = e\varphi_W/T_e$, $\widetilde{V}_p = V_p/V_{te}$, $\widetilde{\omega}_{pj} = \omega_{pj}/\omega_{pi}$, $\widetilde{Z} = Z/\lambda_{De}$, $\widetilde{C}_{si} = C_{si}/V_{te}$, where $C_{si} = \lambda_{De}\omega_{pi}(1-\alpha)^{-1/2}$. First, we shall investigate the potential distributions (via, $\widetilde{\varphi}_D$ and $\widetilde{\varphi}_W$) that may propagate in $Xe^+ - F^- - SF_6^-$ plasma. Therefore, $m_i = 131\ m_p$ (mass of Xe^+), $m_1 = 19\ m_p$ (mass of F^-), and $m_2 = 146\ m_p$ (mass of SF_6^-), where m_p is the mass of proton. Figure 1 displays the normalized Debye–Hückel potential $\widetilde{\varphi}_D$ against the normalized distance $\widetilde{Z}$ for different values of total negative ion concentration α. It is obvious that increasing the total negative ion concentration α leads to reduction in the Debye–Hückel potential. The same behavior is presented for the increase of the electron-to-ion temperature ratio θ. Figures 2–4 display the normalized wakefield potential $\widetilde{\varphi}_W$ against the normalized distance $\widetilde{Z}$ for different values of total negative ion concentration α, density rate of the second negative ion v, and electron-to-ion temperature ratio θ, respectively. When the test charge speed is comparable to the ion-acoustic speed, then regions of negative and positive wakefield potential could appear. The latter is produced behind the test charge and it is clear that the wakefield potential slowly damps on the normalized $\widetilde{Z}$-axis. Furthermore, it is important to note here that an attractive wakefield potential can dominate over the Debye screening potential because of the rapid decrease in the latter beyond the shielding cloud. It is seen that the amplitudes of the wakefield potential are pronounced with the increase of total negative ion concentration α, density rate of the second negative ion v, and electron-to-ion temperature ratio θ. However, at certain values of $\alpha = \alpha_c \approx 0.5, v = v_c \approx 0.91$, and $\theta = \theta_c \approx 8$, the wakefield potential becomes weaker with further enhancement

https://doi.org/10.1017/S0022377811000055 Published online by Cambridge University Press

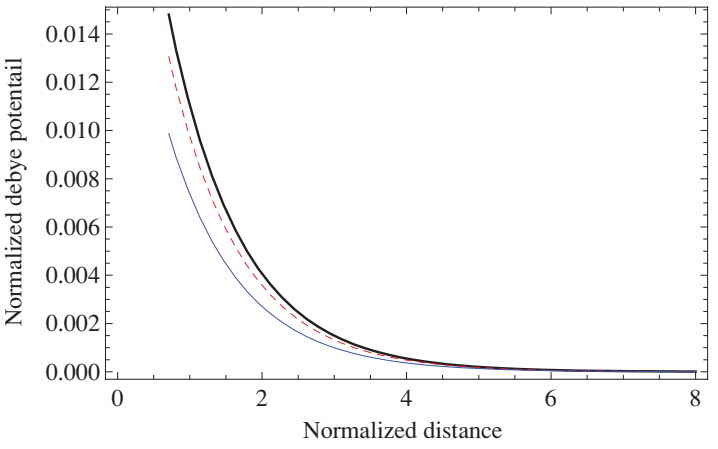


Figure 1. (Color online) The normalized Debye–Hückel potential ($e\varphi_D/T_e$) is plotted against the normalized axial distance (Z/λ_{De}) for different values of the total negative ion concentration $\alpha = 0.1$ (solid–thick curve), $\alpha = 0.3$ (dashed curve), and $\alpha = 0.6$ (solid–thin curve). Here, $\nu = 0.5$ and $\theta = 10$.

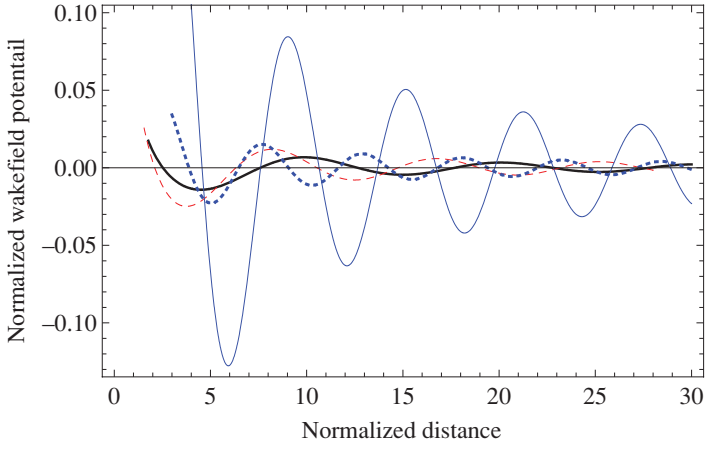


Figure 2. (Color online) For $Xe^+ - F^- - SF_6^-$ plasma, the normalized wakefield potential ($e\varphi_W/T_e$) is plotted against the normalized axial distance (Z/λ_{De}) for different values of the total negative ion concentration $\alpha = 0.1$ (solid–thick curve), $\alpha = 0.2$ (dashed–thin curve), $\alpha = 0.4$ (solid–thin curve), and $\alpha = 0.5$ (dashed–thick curve). Here, $\nu = 0.5$ and $\theta = 10$.

of α, ν, and θ. Similarly, we shall investigate the wakefield potential $\widetilde{\varphi}_W$, which may propagate in $Ar^+ - F^- - SF_6^-$ plasma. The latter has $m_i = 40\ m_p$ (mass of Ar^+), and m_1 and m_2 are given above. Figures 5–7 display the normalized wakefield potential $\widetilde{\varphi}_W$ against the normalized distance $\widetilde{Z}$ for different values of total negative ion concentration α, density rate of the second negative ion ν, and electron-to-ion temperature ratio θ, respectively. One can obviously note that the amplitudes of the wakefield potential are pronounced with the increase of total negative ion concentration α and electron-to-ion temperature ratio θ. Again, at critical values of $\alpha = \alpha_c \approx 0.63$ and $\theta = \theta_c \approx 14$, the wakefield potential amplitude shrinks with

https://doi.org/10.1017/S0022377811000055 Published online by Cambridge University Press

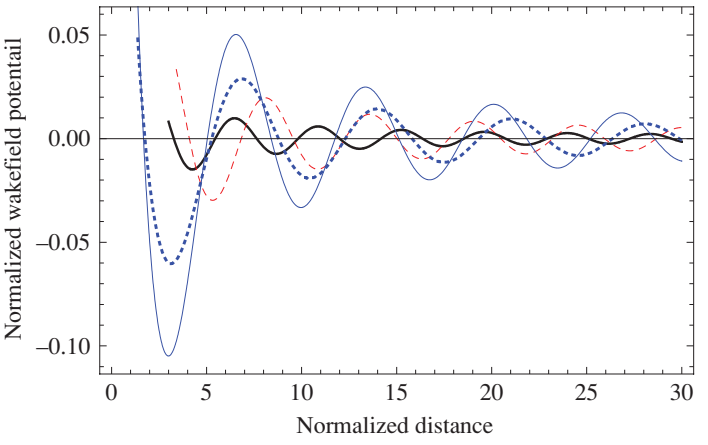


Figure 3. (Color online) For $Xe^{+} - F^{-} - SF_6^{-}$ plasma, the normalized wakefield potential ($e\varphi_W/T_e$) is plotted against the normalized axial distance (Z/λ_{De}) for different values of the density rate of the second negative ion $\nu = 0.1$ (solid–thick curve), $\nu = 0.6$ (dashed–thin curve), $\nu = 0.9$ (solid–thin curve), and $\nu = 0.91$ (dashed–thick curve). Here, $\alpha = 0.5$ and $\theta = 10$.

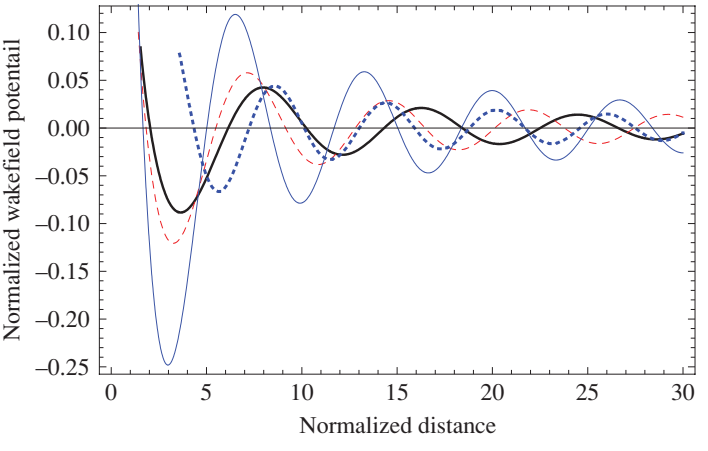


Figure 4. (Color online) For $Xe^{+} - F^{-} - SF_6^{-}$ plasma, the normalized wakefield potential ($e\varphi_W/T_e$) is plotted against the normalized axial distance (Z/λ_{De}) for different values of the electron-to-ion temperature ratio $\theta = 4$ (solid–thick curve), $\theta = 5$ (dashed–thin curve), $\theta = 6$ (solid–thin curve), and $\theta = 8$ (dashed–thick curve). Here, $\alpha = \nu = 0.5$.

the increase of α and θ. However, the strength of the wakefield potential decreases gradually with the increase in the density rate of the second negative ion ν. It is worth mentioning here that the positive and negative regions of the wakefield potentials may help in attracting the same polarity charges and forming ordered crystalline structures in multiion plasmas.

4. Conclusion

In this paper, we have presented a study of the test charge propagation in the presence of ion-acoustic waves in an unmagnetized multicomponent plasma

https://doi.org/10.1017/S0022377811000055 Published online by Cambridge University Press

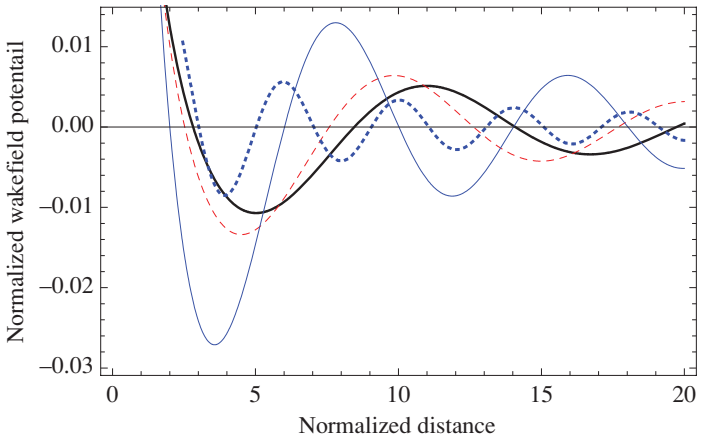


Figure 5. (Color online) For $Ar^+ - F^- - SF_6^-$ plasma, the normalized wakefield potential ($e\varphi_W/T_e$) is plotted against the normalized axial distance (Z/λ_{De}) for different values of the total negative ion concentration $\alpha = 0.1$ (solid–thick curve), $\alpha = 0.2$ (dashed–thin curve), $\alpha = 0.4$ (solid–thin curve), and $\alpha = 0.64$ (dashed–thick curve). Here, $\nu = 0.5$ and $\theta = 10$.

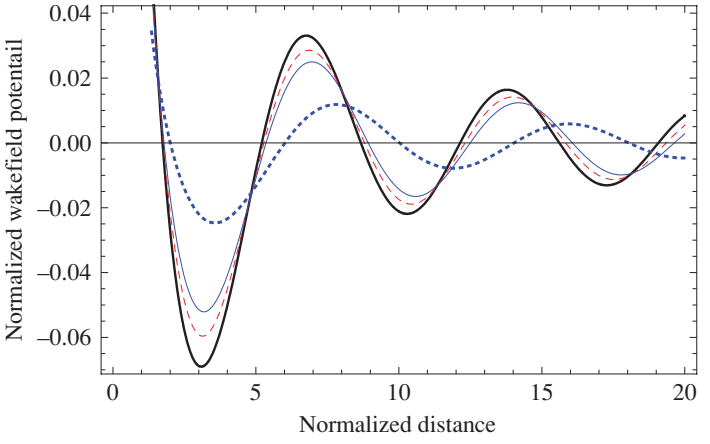


Figure 6. (Color online) For $Ar^+ - F^- - SF_6^-$ plasma, the normalized wakefield potential ($e\varphi_W/T_e$) is plotted against the normalized axial distance (Z/λ_{De}) for different values of the density rate of the second negative ion $\nu = 0.45$ (solid–thick curve), $\nu = 0.5$ (dashed–thin curve), $\nu = 0.55$ (solid–thin curve), and $\nu = 0.9$ (dashed–thick curve). Here, $\alpha = 0.5$ and $\theta = 10$.

consisting of Boltzmann-distributed electrons, positive ions, and two negative ion species. By using the linearized Vlasov equation with Poisson equation, a modified dielectric response function involving the collective mode ion-acoustic waves is derived and used to obtain expressions for the Debye–Hückel and wakefield potentials. The latter is derived in the long wavelength limit in comparison to the normalized radial distance. It is found that the effects of the total negative ion concentration, density rate of the second negative ion, and electron-to-ion temperature ratio have strongly modified both analytical and numerical results of the Debye–Hückel and wakefield potentials. Finally, the present results could

https://doi.org/10.1017/S0022377811000055 Published online by Cambridge University Press

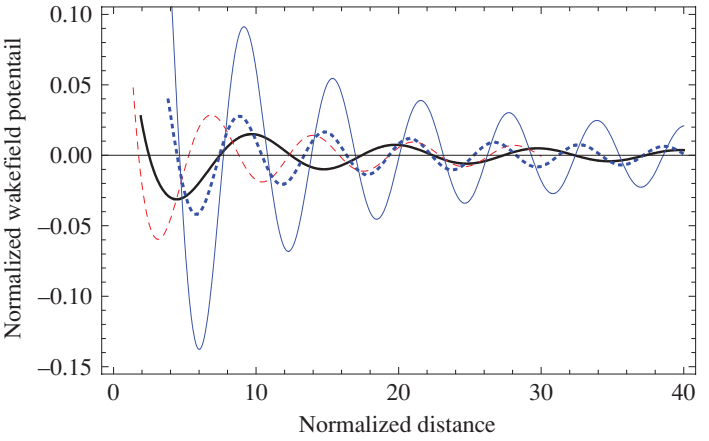


Figure 7. (Color online) For $Ar^+ - F^- - SF_6^-$ plasma, the normalized wakefield potential ($e\varphi_W/T_e$) is plotted against the normalized axial distance (Z/λ_{De}) for different values of the electron-to-ion temperature ratio $\theta = 5$ (solid–thick curve), $\theta = 10$ (dashed–thin curve), $\theta = 13$ (solid–thin curve), and $\theta = 14$ (dashed–thick curve). Here, $\alpha = \nu = 0.5$.

elucidate the test charge properties in plasmas containing two negative ion species, which are important in the context of new material formation in laboratory and negative ion coagulation/agglomeration in space plasmas where the negative ions necessarily exist.

References

[1] Massey, H. S. W. 1976 *Negative Ions,* 3rd edn. Cambridge: Cambridge University Press, p. 663.
[2] Swider, W. 1988 *Ionospheric Modeling*, (ed. J. N. Korenkov). Basel: Birkhauser, p. 403.
[3] Portnyagin, Y. I., Klyuev, O. F., Shidlovsky, A. A., Evdokimov, A. N., Buzdigar, T. W., Matukhin, P. G., Pasynkov, S. G., Shamshev, K. N., Sokolov, V. V. and Semkin, N. D. 1991 *Adv. Space Res.* **11**, 89.
[4] Chaizy, P. H., Rème, H., Sauvaud, J. A., D'uston, C., Lin, R. P., Larson, D. E., Mitchell, D. L., Anderson, K. A., Carlson, C. W., Korth, A. and Mendis, D. A. 1991 *Nature (London)* **349**, 393.
[5] Coates, A. J., Crary, F. J., Lewis, G. R., Young, D. T., Waite, J. H. Jr. and Sittler, E. C. Jr. 2007 *Geophys. Res. Lett*. **34**, L22103.
[6] Nakamura, Y., Nakamura, M. and Itoh, T. 1976 *Phys. Rev. Lett*. **37**, 209.
[7] Tran, M. Q. and Coquerand, S. 1976 *Phys. Rev.* A **14**, 2301.
[8] Wong, A. Y., Mamas, D. L. and Arnush, D. 1975 *Phys. Fluids* **18**, 1489.
[9] Ahearn, A. J. and Hannay, N. B. 1953 *J. Chem. Phys.* **21**, 119.
[10] Song, B., D'Angelo, N. and Merlino, R. L. 1991 *Phys. Fluids* B **3**, 284.
[11] Sato, N. 1994 *Plasma Sources Sci. Technol.* **3**, 395.
[12] Koga, K. and Kawai, Y. 1999 *Japan. J. Appl. Phys.* **38**, 1553.
[13] Nakamura, Y., Bailung, H. and Lonngren, K. E. 1999 *Phys. Plasmas* **6**, 3466.
[14] Nakamura, Y., Odagiri, T. and Tsukabayashi, I. 1997 *Plasma Phys. Control. Fusion* **39**, 105.
[15] Ludwig, G. O., Ferreira, J. L. and Nakamura, Y. 1984 *Phys. Rev. Lett*. **52**, 275.

https://doi.org/10.1017/S0022377811000055 Published online by Cambridge University Press

[16] Wong, A. Y., Mamas, D. L. and Arnush, D. 1975 *Phys. Fluids* **18**, 1489.

[17] Das, G. C. 1979 *Plasma Phys.* **21**, 257; Das, G. C. and Singh, Kh. I. 1991 *Aust. J. Phys.* **44**, 523.

[18] Moslem, W. M. 1999 *J. Plasma Phys.* **61**, 177; Moslem, W. M. 2000 *J. Plasma Phys.* **63**, 139; El-Labany, S. K., El-Warraki, S. A. and Moslem, W. M. 2000 *J. Plasma Phys.* **63**, 343.

[19] Ichiki, R., Yoshimura, S., Watanabe, T., Nakamura, Y. and Kawai, Y. 2002 *Phys. Plasmas* **9**, 4481.

[20] Singh, D. K. and Malik, H. K. 2008 *IEEE Trans. Plasma Sci.* **36**, 462; Malik, H. K. and Stroth, U. 2008 *Plasma Sources Sci. Technol.* **17**, 035005.

[21] Sabry, R., Moslem, W. M. and Shukla, P. K. 2009 *Phys. Plasmas* **16**, 032302; Moslem, W. M., Abdelsalam, U. M., Sabry, R. and Shukla, P. K. 2010 *New J. Phys.* **12**, 073010; Moslem, W. M., Abdelsalam, U. M., Sabry, R., El-Shamy, E. F., and El-Labany, S. K. 2010 *J. Plasma Phys.* **76**, 453.

[22] Mamun, A. A., Shukla, P. K. and Eliasson, B. 2009 *Phys. Rev.* E, **80**, 046406; Sharma, S. K. and Bailunga, H. 2010 *Phys. Plasmas* **17**, 032301.

[23] Ichiki, R., Shindo, M., Yoshimura, S., Watanabe, T. and Kawai, Y. 2001 *Phys. Plasmas* **8**, 4275.

[24] Coates, A. J., Crary, F. J., Lewis, G. R., Young, D. T., Waite, J. H. Jr., Sittler, E. C. Jr. 2007 *Geophys. Res. Lett.* **34**, L22103.

[25] Neufeld, J. and Ritchie, R. H. 1955 *Phys. Rev.* **98**, 1632.

[26] Sanmartin, J. R. and Lam, S. H. 1971 *Phys. Fluids* **14**, 62.

[27] Chen, L., Langdon, A. B. and Lieberman, M. A. 1973 *J. Plasma Phys.* **9**, 311.

[28] Nambu, M. and Akama, H. 1985 *Phys. Fluids* **28**, 2300.

[29] Ishihara, O. and Vladimirov, S. V. 1997 *Phys. Plasmas* **4**, 69; Ishihara, O., Vladimirov, S. V. and Cramer, N. F. 2000 *Phys. Rev.* E **61**, 7246.

[30] Salimullaha, M. and Shukla, P. K. 1998 *Phys. Plasmas* **5**, 4205; Nambu, M., Salimullah, M. and Bingham, R. 2001 *Phys. Rev.* E **63**, 056403.

[31] Kourakis, I. and Shukla, P. K. 2003 *Phys. Lett.* A **317**, 156; Shukla, P. K. and Eliasson, B. 2008 *Phys. Lett.* A **372**, 2897.

[32] Shukla, P. K. and Stenflo, L. 2001 *Plasma Phys. Rep.* **27**, 904.

[33] Ali, S., Nasim, M. H. and Murtaza, G. 2003 *Phys. Plasmas* 10, 4207; Ali, S., Murtaza, G. and Nasim, M. H. 2005 *Phys. Plasmas* **12**, 072104; Ali, S., Murtaza, G. and Nasim, M. H. 2005 *Phys. Plasmas* **12**, 072104.

[34] Ali, S., Moslem, W. M. and Shukla, P. K. 2008 *Phys. Lett.* A, **372**, 6650; Ali, S. and Shukla, P. K. 2008 *Phys. Lett.* A **372**, 4827; Ali, S. 2009 *Phys. Plasmas* **16**, 054502; Ali, S. 2009 *Phys. Plasmas* **16**, 113706.

https://doi.org/10.1017/S0022377811000055 Published online by Cambridge University Press